ISSN 1392 - 1207. MECHANIKA. 2005. Nr.5(55)

Features of stress strain state in specimen neck at (when) computationally modeling a tension process

V. Bagmutov*, S. Babichev**
**Volgograd State Technical University, 28 Lenin Ave., 400131 Volgograd, Russia, E-mail: sopromat@vstu.ru*
***Kamyshin Technological Institute (branch) The Volgograd State Technical University, 6a Lenin Str., 403870 Kamyshin, Russia, E-mail: sapr@kti.ru*

1. Introduction

The solution of a problem on deformations localization when a specimen is under tension is important, first of all, from the viewpoint of plasticity resource estimation under complex stress. The known approaches of Bridgman P., Siebel E., Davidenkov N. and Spiridonova N. [1, 2] describe stress-strain state (SSS) not in the entire neck volume, but in its least section, and for this purpose it is necessary to have curvature radius the neck R in meridional section and its least diameter d_N at intermediate stages of deformation, except for the finishing one. The problem of modeling process of a specimen neck formation under tension is interesting in theoretical and applied aspects. Knowing the evolution of SSS at the stage of deformation concentration in a sufficiently narrow area (in comparison with the working length of the specimen) helps to obtain additional data on the influence of the stress state type on plastic deformation ability of the material plasticity resource evaluation up to the specimen full rupture to determine SSS parameters influencing the crack initiation process.

2. Testing procedures

The given work considers the issues concerned with analyzing the results of computational modeling of formation process of a cylindrical specimen neck at all stages of occurrence and development up to failure on the basis of the neck formation model, stated in papers [3-5]. Computational experiment on the basis of the offered model of elastoplastic behaviour of a cylindrical specimen under tension allows to describe stress state at any point of the given neck formation area at all stages of the specimen deformation. For its realization it is necessary to lean on the results of real tests, since the necessary initial information to start a neck formation model is the experimental machine diagram of tension in coordinates: force F – elongation Δl and (or) the diagram in coordinates $F - \psi$, where ψ is percentage reduction of the area. That is, three variants of computational experiment realization are possible depending on the type of initial diagram: 1) if diagrams $F - \Delta l$ and $F - \psi$ are available; 2) – diagram F - ψ ; 3) – diagram $F - \Delta l$.

The research of neck formation process was carried out by the example of cylindrical specimens from steel 35, 80 and titanium alloy PT5V.

In accordance with this model Fig. 1 shows the drawing of a concentrated elastoplastic deformation zone (area *"N"*) and elastic deformation (area *"E"*) arrangement and some geometrical parameters (control parameters CP), determining plastic deformation area at any stage of neck development through the configuration definition of line *ABC* of the *"N"* and *"E"* areas boundary (characteristic types of lines *ABC* meet on Fig. 1 j = 1, 2, 3).

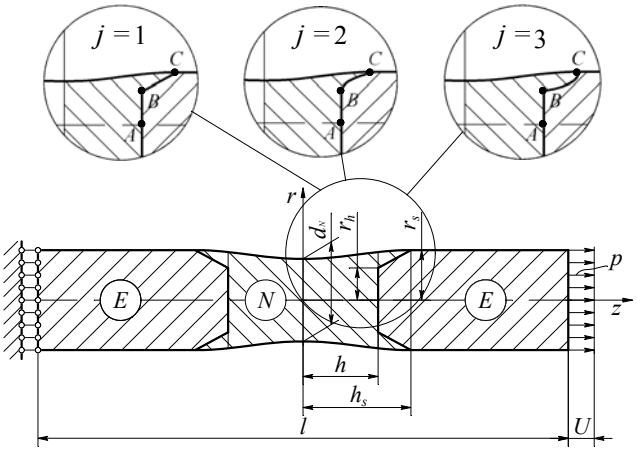

Fig. 1 Loading diagram of neck formation in a specimen and variants of the *"N"* and *"E"* area boundary

The model of neck formation given in Fig. 1 is mathematically described as follows:

- area of elastic deformations *"E"*

$$\sigma_i = E \cdot \varepsilon_i, \quad \forall (r,z) \in \Omega_E \tag{1}$$

- area of elastoplastic deformations *"N"*

$$S_i = S_i(e_i), \quad \forall (r,z) \in \Omega_N \tag{2}$$

here and further r is radius, z is longitudinal axis of the specimen, σ_i, ε_i, S_i, e_i are engineering and true stress and strain, E is Jung's module. Index i means stress or strain intensity

- the partition boundary B_{N-E} of areas *"N-E"*, described by lines *ABC* (Fig. 1)

$$r = f(z), \quad \forall (r,z) \in B_{N-E} \tag{3}$$

In the view of unequal involvement degree of various layers in the process of plastic deformation after neck initiation the meridional cross-sectional surfaces of *"N"* and *"E"* parts are represented on a section half by *AB* and *BC* lines (Fig. 1). To reduce the quantity of control parameters when representing different variants of lines *BC* square-law general view dependence is used in the system *r-z*:

$$r=\left(tg\,\alpha_1-tg\,\alpha_j\right)\frac{(z-h)^2}{(h_s-h)}+(z-h)tg\,\alpha_j+r_h,\ j=1,\ 2,\ 3 \qquad (4)$$

when j=1 the equation (4) describes straight line BC, i.e.

$$r=(z-h)\ tg\,\alpha_1+r_h \qquad (5)$$

Proceeding from Fig. 1

$$tg\,\alpha_1=\left(r_s-r_h\right)\left(h_s-h\right)^{-1} \qquad (6)$$

For j=2 $tg\ \alpha_j < tg\ \alpha_1$; for j=3 $tg\ \alpha_j > tg\ \alpha_1$; here when $z=h$ $dr/dz=tg\ \alpha_j$;
when

$$z=h_s\ \ tg\,\alpha_h=dr/dz=2tg\,\alpha_1-tg\,\alpha_j,\ 0\le\alpha\le\pi/2 \qquad (7)$$

Maximum quantity CP for j =1 includes: h, r_h, $tg\ \alpha_1$; for j=2, 3: h, r_h, h_s, $tg\ \alpha_j$, $tg\ \alpha_1$.

Relative residual deformations are connected in the uniform deformation area by the known dependences

$$e=ln\left(1-\psi\right)^{-1} \quad \text{or} \quad \psi=1-\left(exp\,e\right)^{-1} \qquad (8)$$

To adjust the model (1)-(7) more exactly and thereby to give a more authentic description of the SSS specimen in the *"N"* neck area it is desirable at one or several tension stages, including the final one, to have photos of the specimen or gaugings of the neck diameters d_N along the axis z.

Adjustment of the model realized with the use of the finite element method (FEM), is made at fixed tension magnitudes. Tension magnitude is defined by longitudinally moving the right end of the specimen U working part in the length l, by selecting both the form of the *"N"* and *"E"* areas boundary, i.e. lines ABC, and the optimal grid topography and finite elements (FE) configuration in the specimen loading diagram. $U=\Delta l$ is defined as a part of the specimen length increment of $U_k=l_k-l_u$ between final length l_k and the length l_u at the moment of achieving the greatest uniform deformation.

Transition to the model of the *"N - E"* compound composition of the neck specimen is realized when the greatest value of force F_u appropriate to tensile strength σ_u,

$$\sigma_u=4F_u\left(\pi\,d_0^{\,2}\right)^{-1} \qquad (9)$$

and also the values e_u is relative longitudinal uniform residual deformation and ψ_u is uniform residual cross-sectional contraction, connected among themselves by dependence (8), are achieved [3].

At the first stage of tension (when n = 1 and $U=U_1$) the distance $h=h_1=h_1^{\,t}$ along axis z from the neck center (z = 0) up to the *"N - E"* area boundary with the use of the work results [1, 2] is defined as follows

$$h_1^t=\sqrt{R_0\left(2r_u-d_{N0}\right)},\ \ R_0=d_{N0}\left(1.56\left(e_1-e_u\right)\right)^{-1} \qquad (10)$$

where r_u is a radius corresponding to size e_u; d_{N0} is a diameter of the minimal neck cross-section $d_{N0}=d_0\sqrt{1-\psi_1}$; ψ_1 is calculated with the use of the dependence (8) and the size $e_1=ln\left(1+U_1/l_0\right)$, where l_0, d_0 are initial length and diameter of the specimen.

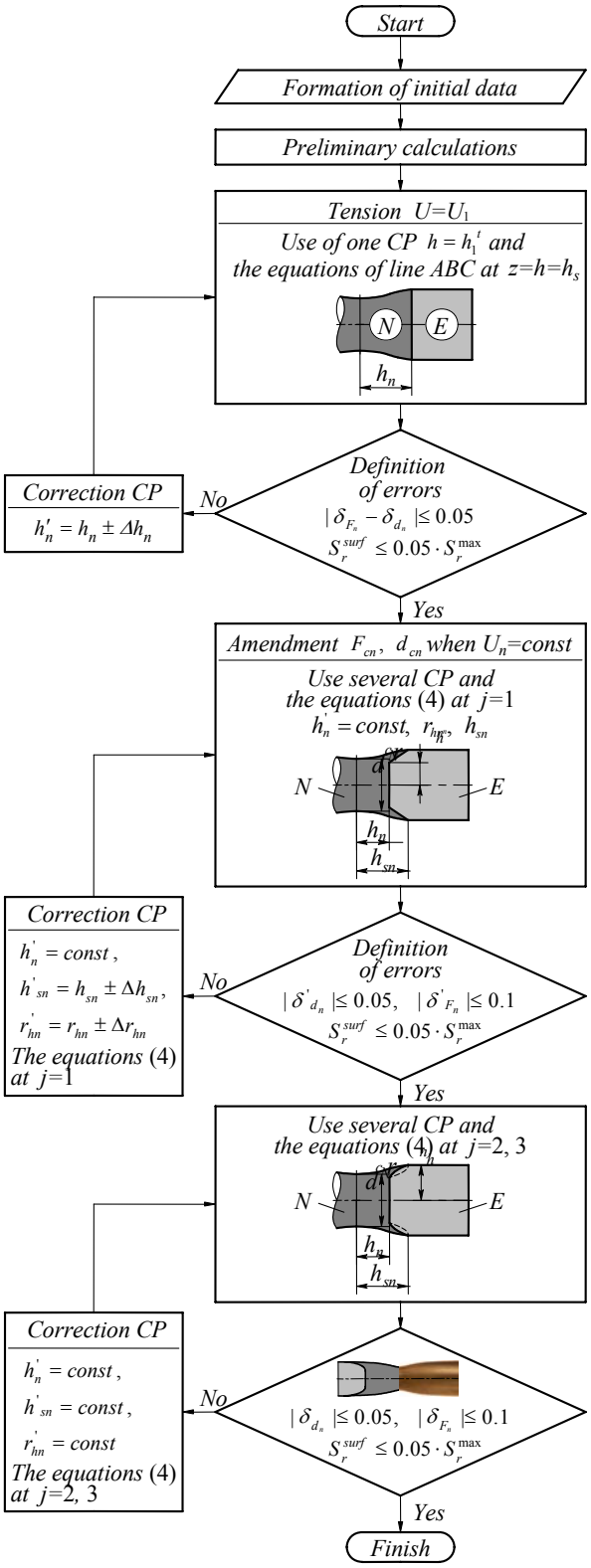

Fig. 2 Algorithm of carrying out computational experiment at any n-th stage of tension

As the first approximation it is accepted, that the *"N - E"* area boundaries coincide with the specimen cross-section on the distances h_1 from z = 0, i.e. the ABC line equation $z=h=h_s$.

According to the algorithm of carrying out computational experiment (Fig. 2), and accepted at the given stage of tension of area *"N"* the force at movable end surface of the specimen F_1 and the diameter in the least section of neck d_N are defined. Tension diagrams being available F - Δl and F - ψ are compared to the experiment and the sizes d_N, F are specified due to a variation in the iterative mode of the model h parameter. Let us notice, that the force error at end face δ_F depends on parameter h in the greater degree, than the diameter error (in recalculation through ψ) in the least neck section δ_d.

The parameter $h = h_1^t$ (further, to simplify the record, the iteration number in the used sizes is not indicated), limiting the area of neck localization, sets a border to the simplified neck model [1], being different from the real one (Fig. 3). As shows the computational experiment parameter h' corrected as a result of an iterative process considerably exceeds the values obtained in theoretical way by formulae (10) and can vary (see Fig. 4). The overestimated value h' results from a smoother neck configuration and, accordingly, from a bigger plastic volume involved in the neck formation area, than given in paper [1].

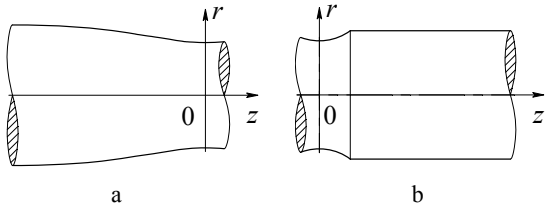

Fig. 3 Difference of real neck configuration (a) and the neck model obtained as a result of work [1] (b)

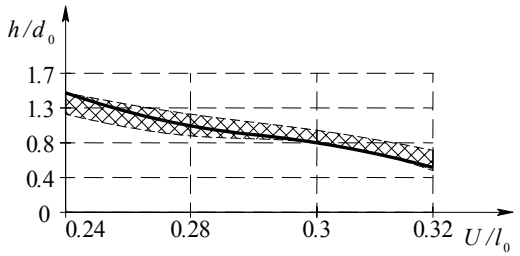

Fig. 4 Main CP h change range at all stages of neck development, up to breaking (continuous line shows the change of optimum parameter h for the specimen from steel 35)

The diagram F - ψ being unavailable the model (1)-(7) adjustment is made only by using size F and diagram F - Δl. The iterative process stops when conditions are met

$$| \delta_d | \le 0.05 ; | \delta_F | \le 0.1 ; \; S_r^{surf} \le 0.05 \, S_r^{max} \qquad (11)$$

here S_r^{surf}, S_r^{max} are radial stress determined on the surface (an index *"surf"*) and on the specimen axis z (an index *"max"*) in the least neck section.

Experimentally revealed configuration of a meridional neck section, or its photos being available, error δ_d is specified in some cross-sections of a half of area *"N"* with introduction of subset (CP) $\subset$ {CP}, where the set {CP} is defined by a full set of five elements. In this case, parameters variation of a subset in the set on intervals

$$\begin{cases} 0 < d_N < 2\, r_u; \\ 0 \le \alpha_j \le \pi/2; \\ 0 < h \le h_s < l/2; \\ j = 1, 2, 3 \end{cases}$$

is defined from the condition of evasion degree minimization of the calculated longitudinal specimen section from the experimental one, simultaneously checking the performance of the conditions (11) (Fig. 5).

At the end of model adaptation on n-th tension stage, transition is made to the following tension stage, with a new value $U_{n+1} = U_n + \Delta U$ assigned; $0 < \Delta U \le U_k$ for which all operations are repeated, and their value at previous tension stage is accepted as CP reference values.

Trustworthy information on neck configuration being unavailable, the opportunity of level δ_F, δ_d minimization is checked by modifying parameters from subsets (CP). The choice of subsets is made according to the sequence number of curves BC (j = 1, 2, 3). The variation of parameters in the space of the chosen subset (CP) is carried out using the generator of random numbers. However, it does not mean, that arbitrarily chosen values (from the CP change ranges revealed by preliminary calculations) will give allowable errors δ_F and δ_d. I.e., a combination of parameters from CP set is necessary within the limits of every tension stage.

To reduce the CP disorder it is recommended to observe the sequence when transferring from the initial tension stage down to the moment of breaking.

At the final stage formation of the dependence of all CP on the magnitude of tension stage U is carried out, i.e. the formation of control functions $CP = CP(U)$ (Fig. 6) is made.

The reliability of received results depends, first of all, on initial data completeness. The greatest accuracy is a characteristic of realization variant of computational experiment 1 and the presence of neck configuration in the meridional section. The least one is characteristic of variant 3 since diagram F - ψ being unavailable, the model adjustment is made only using parameter F and diagrams F - Δl.

The error of the force at movable end surface δ_F and the diameter in the least neck δ_d section increases pro-

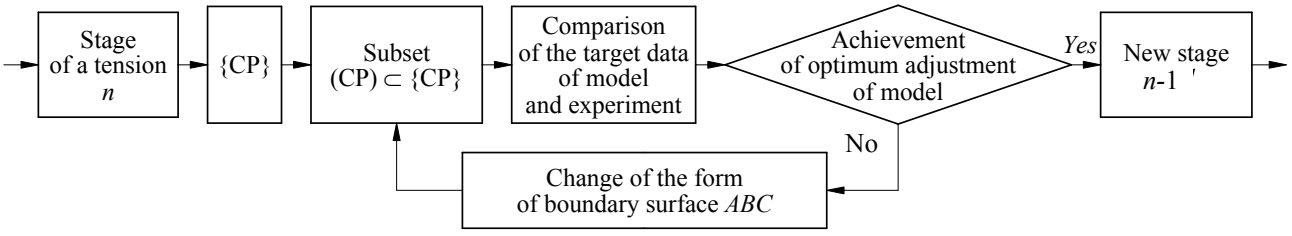

Fig. 5 Procedure of model adaptation at the n-th tension stage of a specimen with a neck

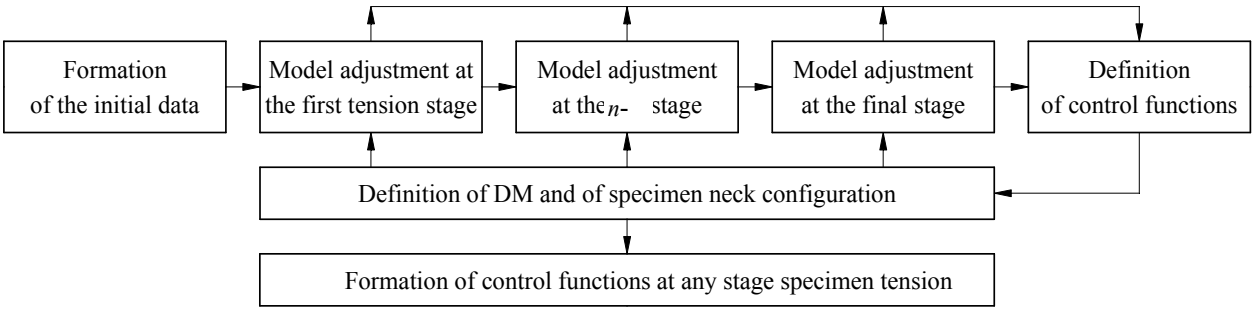

Fig. 6 The control function definition diagram at all stages of neck specimen deformation

portionally to the increase in tension stage and will be the greatest at the moment of failure. The comparison result of full calculated and experimental diagrams F - ψ for a specimen from steel 35 has shown the greatest deviation of diameter d_N less than 5 %, and the greatest deviation of force F at the movable end surface – less than 9 % (Fig. 7).

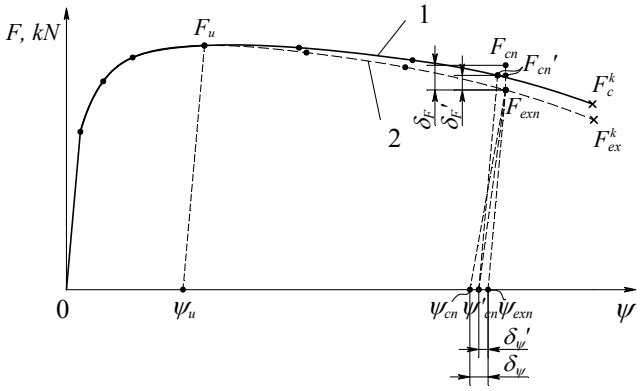

Fig. 7 Comparison of the full calculation diagram of tension *1* with experimental *2* for steel 35 and definition of errors δ_F and δ_ψ at the n-th stage of tension, where F_{ex}, ψ_{ex} are experimental values; F_c, ψ_c are calculated values; F_c', ψ_c' are the specified calculated values as iterative process result

Fig. 8 shows the evolution of stress (a) and strain state (b) in the least specimen neck section in radial and circumferential directions at all tension stages, up to the final one (n = 4). Fig. 9 shows the change in the stress intensity picture S_i and of the topology of finite element grid (analogue to a reference grid) at the stages of tension n = 1-4 for the site allocated from area "*N*" with equal number FE.

Fig. 10 shows a comparison of axial S_z, radial S_r and tangential S_θ stresses obtained with the use of model (1)-(7) and the formulas of N. Davidenkov and N. Spiridonova [6] (according to the accepted table of symbols)

$$\left.\begin{aligned} S_r &= S_i \frac{d_N}{4R}\left(1-\frac{r_m^{\,2}}{\left(d_N/2\right)^2}\right) \\ S_z &= S_i\left(1+\frac{d_N}{4R}-\frac{r_m^{\,2}}{d_N R}\right) \end{aligned}\right\} \qquad (12)$$

where stress intensity

$$S_i = \frac{F}{\pi\left(d_N/2\right)^2\left(1+d_N/(8R)\right)}$$

here d_N is the least neck diameter; R is curvature radius in the meridional neck section; r_m is radius change in the least neck section; F is the force at the end face.

Fig. 11 shows the calculated neck configuration in comparison with the experimental one and the distribution of stress intensity S_i in the elastoplastic volume along the specimen axis using a 9-th level stress scale.

In the conclusion it is necessary to note, that the technique stated above has been checked up for materials with various value of percentage of area reduction ψ, describing plasticity measure (Table).

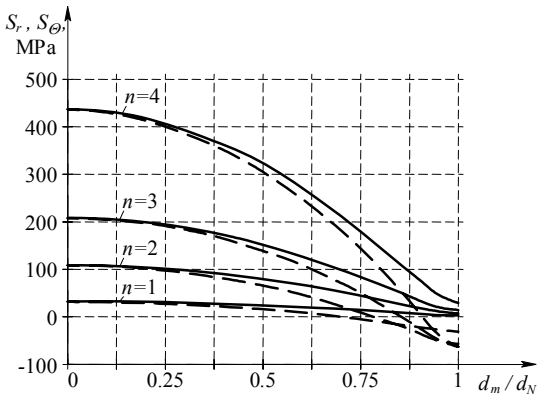

a

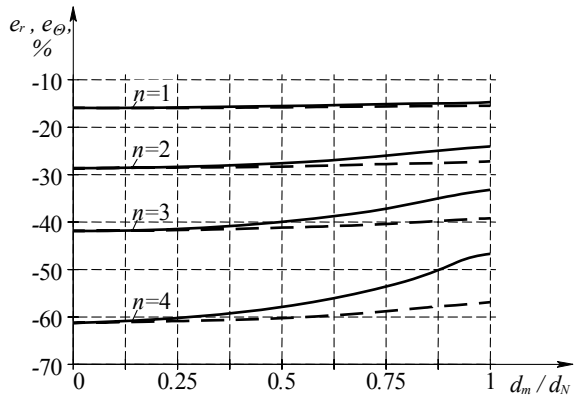

b

Fig. 8 Distribution of radial S_r, e_r (continuous lines) and tangential S_Θ, e_Θ (dotted) stress (a) and strain (b) along neck radius (d_m is current radius, d_N is the radius on the contour of least neck section) at tension stages n = 1-4

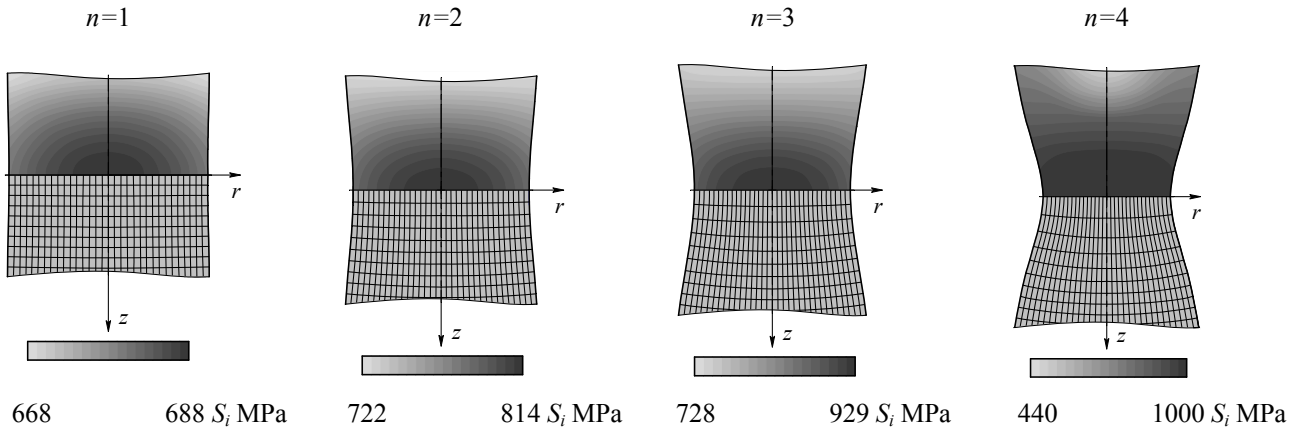

Fig. 9 Change of a stress intensity picture S_i using 18-level scales and grid topology FE depending on the tension stage

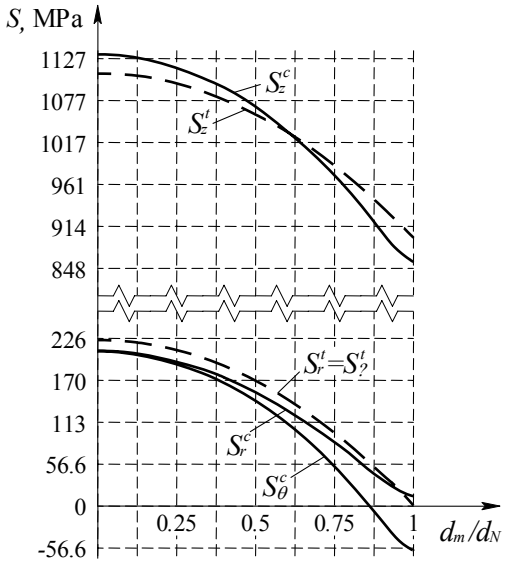

Fig. 10 Comparison of axial, radial and tangential stress obtained using model (1)-(7) (an index *"c"*) and formulas (12) (an index *"t"*) for the tension stage n = 3 (penultimate before breaking)

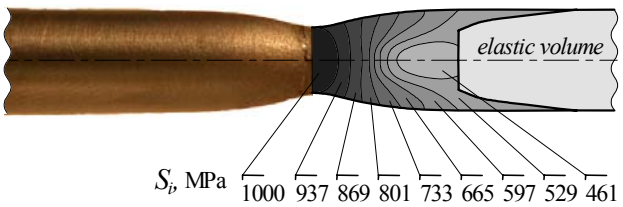

Fig. 11 Comparison of the calculated neck configuration (on the right) with the photo of real specimen (on the left) and stress intensity S_i fields at the moment of failure

Table

Mechanical properties of materials

	Kind of the initial diagram	$\sigma_{0.2}$	σ_u	C_ψ	ψ_k, %
		MPa			
Steel 80	F - Δl	764	1182	1586	34.4
Steel 35	F - ψ	185	511	1005	64.6
Titanium alloy PT5V	F - Δl, F - ψ	810	904	1192	37.5

The results of computational experiments for the mentioned above materials have shown, that the greatest adjustment accuracy of model (1)-(7) is reached for materials which have a more expressed configuration of the neck and have larger ψ. However, the given conclusion characterizes an ability of the model (1)-(7) to adapt to the change of geometrical parameters and the parameters of specimen plasticity, and the accuracy of the obtained results in greater degrees depends on the accuracy of experimental data.

3. Conclusions

1. This research offers principles of computational modeling on the basis of finite element method of a cylindrical specimen neck formation at all stages of its development, up to the specimen failure.

2. Neck formation model adaptation procedures are described and recommendations on their application are given.

3. The analysis of mode evolution of the neck area deformation is made during the specimen tension.

4. Comparison of the results of computational modeling with known analytical dependences is made.

5. Comparison of the calculated and experimental data is made for materials with various initial data and parameters of plasticity.

References

1. **Давиденков Н.Н., Спиридонова Н.И.**-Заводская лаборатория. 1945, т.X1, No6. с.583-593.
2. **Кутяйкин В.Г.** Диагностика материалов.-Заводская лаборатория. 2002, т.68, No9, с.53-55.
3. **Багмутов В.П., Бабичев С.В.** Моделирование процесса формирования шейки цилиндрического образца при растяжении.-XXIV Российская школа по проблемам науки и технологий, посвященная 80-летию со дня рождения академика В.П. Макеева. Краткие сообщения. -Екатеринбург: УрО РАН, 2004, с.185-187.
4. **Bagmutov, V., Babichev, S.** Computational modeling of process of elastoplastic straining of a specimen with a neck under tension.- Mechanika-2005.-Proc. of the 10 th Int. Conf. April 7-8, 2005 Kaunas University of Technology, Lithuania, p.103-108.
5. **Багмутов В.П., Бабичев С.В.** Адаптация модели

упругопластического деформирования образца с шейкой при реализации вычислительного эксперимента на растяжение.-Материалы III Всероссийской конф., Камышин, 20-22 апреля 2005, т.1, с.33-36.
6. **Малинин Н.Н.** Прикладная теория пластичности и ползучести.-Москва: Машиностроение, 1975.-400с.

V. Bagmutov, C. Babičev

BANDINIO KAKLIUKO ĮTEMPIMŲ IR DEFORMACIJŲ BŪVIO YPATUMAI SKAITMENIŠKAI MODELIUOJANT TEMPIMO PROCESĄ

R e z i u m ė

Papildoma ir tikslinama autorių anksčiau pateikta skaitmeninio modeliavimo baigtiniais elementais cilindrinio bandinio kakliuko susiformavimo visuose raidos etapuose, iki visiško bandinio suirimo metodika. Išnagrinėtos bandinio modelio su kakliuku adaptavimosi procedūros, atlikta įtempių ir deformacijų būvio evoliucijos kakliuko srityje bandinio tempimo metu analizė. Skaitinio modeliavimo rezultatai palyginti su žinomomis analitinėmis priklausomybėmis. Atliktas skaičiavimo ir eksperimentų rezultatų palyginimas.

V. Bagmutov, S. Babichev

FEATURES OF STRESS STRAIN STATE IN SPECIMEN NECK AT (WHEN) COMPUTATIONALLY MODELING A TENSION PROCESS

S u m m a r y

The previously introduced by the authors procedures of computational modelling on the basis of finite element method of a cylindrical specimen neck formation process at all stages of its development, up to the specimen failure is supplemented and specified here. The researchers describe the procedures of a specimen with a neck model adaptation and analyze the evolution of deformation mode in the necking area of the specimen tension process. The results of computational modelling are compared with the known analytical dependences. Comparison of calculated and experimental data are made.

В. Багмутов, С. Бабичев

ОСОБЕННОСТИ НАПРЯЖЕННО-ДЕФОРМИРОВАННОГО СОСТОЯНИЯ В ШЕЙКЕ ОБРАЗЦА ПРИ ЧИСЛЕННОМ МОДЕЛИРОВАНИИ ПРОЦЕССА РАСТЯЖЕНИЯ

Р е з ю м е

Дополняется и уточняется, предложенная ранее авторами, методика численного моделирования на основе метода конечных элементов процесса образования шейки цилиндрического образца на всех этапах ее развития, вплоть до разрушения образца. Рассмотрены процедуры адаптации модели образца с шейкой и сделан анализ эволюции напряженно-деформированного состояния в области шейки в процессе растяжения образца. Сопоставлены результаты численного моделирования с известными аналитическими зависимостями. Произведено сопоставление расчетных и экспериментальных данных.

Received January 31, 2005